LANGMUIR

pubs.acs.org/Langmuir Article

Leakage Retardation of Static Seals via Surface Roughness and Wettability Modification

Zhengpeng Gu,[§] Qingwen Dai,[*,§] Chenbo Ma, Wei Huang, and Xiaolei Wang

Cite This: *Langmuir* 2024, 40, 12842−12851 Read Online

ACCESS | Metrics & More | Article Recommendations | Supporting Information

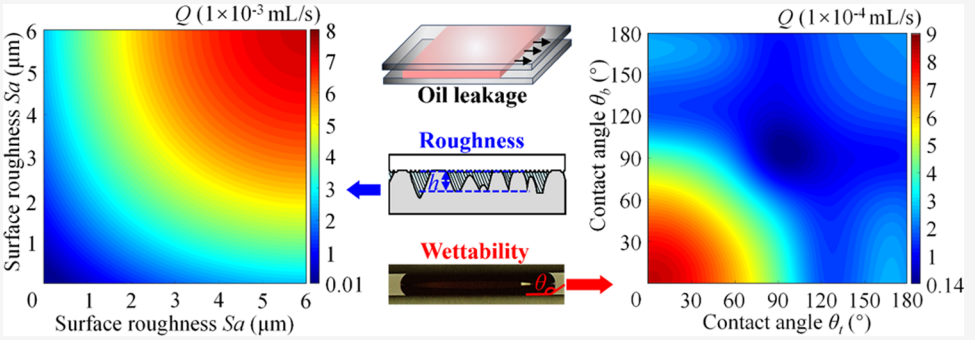

ABSTRACT: In this paper, the effects of surface roughness and wettability on the leakage performance of static seals were highlighted. The results show that the leakage rate is negatively correlated with the contact pressure and positively correlated with surface roughness. Surface wettability affects leakage performance. Leakage retardation is achieved by modifying the roughness and wettability at the interface. The seal interface consists of two oleophobicity surfaces and exhibits an excellent seal performance, of which the leakage reduction is approximately 64%. A theoretical model based on wettability is established to predict the leakage rates under varying wettability conditions, and its validity is confirmed. This research result is expected to be applied in the field of seals and predict the leakage performance of interfaces with different wettabilities to minimize and reduce the leakage of oil in static sealing systems.

INTRODUCTION

Metal static sealing interface consists of two rough surfaces, and the principle is to achieve sealing purposes through the compression and elastic deformation of the metal materials. Due to its outstanding performance of high-pressure bearing capacity, simple structure, high-temperature resistance, and corrosion resistance, metal static sealing is widely used in many applications including aerospace,[1] petrochemical,[2] deep space exploration, etc.[3] There are many factors causing leakage, such as surface material,[4] contact pressure,[5,6] surface roughness,[7] and surface wettability.[8,9] Generally, the leakage of metal static seals would directly affect the operation safety of the device and lead to environmental pollution and a waste of resources. Identifying leakage mechanism and developing antileakage methods are essential to reduce the losses.

Over the past few decades, experimental research on the sealing performance of metal static seals has mainly focused on the influence of surface parameters, material selection, and contact pressure. Zhang et al.[3] measured the leakage rate of static seals under different contact pressures with a high accuracy device. The results showed a negative correlation between the contact pressure and leakage rate. The leakage rate at a contact pressure of 500 N is 43% lower than that of 100 N. Murtagian et al.[5] proposed a sealing parameter weighted area (W_a) that was related to the contact pressure and length and calculated a critical value for which leakage can be determined. Yanagisawa et al.[6] investigated the effect of roughness and contact pressure on leakage and found that the roughness and contact pressure were positively correlated with sealing performance. Goltsberg et al.[7] found that the sealing performance was in positive correlation with the contact pressure and negative correlation with surface roughness. At a contact pressure of 150 MPa, the leakage rate at a surface roughness of 0.8 μm is 10 times higher than that at a surface roughness of 0.2 μm.

In a theoretical aspect, establishing a leakage model to predict the leakage rate is of first importance. Over the past decades, various leakage models were constructed including contact mechanics model[10,11] and leakage channel model considering surface parameters,[12−14] which laid the foundation

Received: March 14, 2024
Revised: May 21, 2024
Accepted: May 21, 2024
Published: June 3, 2024

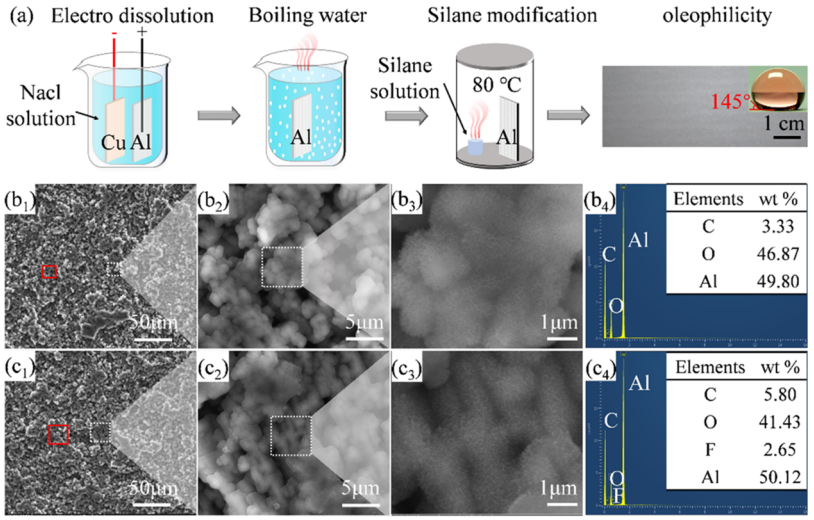

Figure 1. (a) Fabrication process. SEM and EDS images of roughened Al surfaces (R_a = ~2 μm) without (b_1−b_4) and with (c_1−c_4) silane modified for 3 h.

for leakage rate prediction. In the meanwhile, surface multiscale effects,[15−18] contact deformation,[19] the fractal theory,[20] and the percolation theory[21] were considered successively to improve the prediction accuracy. It should be noticed that these models mainly focus on the surface structure parameters due to contact deformation, while its wetting properties are not considered.

Actually, different wettability surfaces also affect the flow state. Chen et al.[22] inspired by the conical structure of a cactus and the kinematic configuration of a centipede proposed an ability to achieve self-transportation of fluids between any surfaces or interfaces by modulating the surface wettability. Qi et al.[23] constructed an array of hydrophilic/hydrophobic stripes on the surface of slippery liquid-infused porous surfaces and applied them to fog collection. The results show that the structure can transport droplets quickly and precisely. Yang et al.[24,25] prepared 3D topological surfaces on Cu substrates by combining the grooved structure of rice leaves and the wedge-shaped structure of a shorebird's beak with droplet transport capability. The created surfaces can not only manipulate droplets of acid, alkali, and salt solutions but also steer droplet sliding/friction. Zhou and Ye et al.[26] used LBM simulations to explore the effect of the wettability of the fracture surface on the two-phase flow characteristics. The results showed that the displacement process is usually more unstable, and the invasion front is more tortuous in a rougher and more wettable fracture, which leads to larger entry pressure and displacement resistance. Ou et al.[8] conducted flow experiments with superhydrophobic microchannels and found that the resistance to flow was reduced by 40%. From the above studies, it is confirmed that surface wettability has a significant effect on the flow of fluids, and the effect of controlling the fluid motion can be achieved by modulating the surface wettability. However, most of the applications of modulating surface wettability have been focused on precise droplet transport, collection, and gripping, but there are a few reports on its application to static sealing. Therefore, it is important to investigate the effect of surface wettability on static seal leakage.

Hence, in this paper, a strategy for delaying leakage by modifying the surface roughness and wettability is proposed. The surfaces with different roughnesses and wettabilities are fabricated, and the effects of surface roughness and wettability on the leakage behavior are discussed. The leakage process and leakage rate were investigated. The leakage process of oil is captured, and its mechanism is revealed. The proposed control strategy is considered to have potential applications in sealing and leakage prevention in modern machinery.

MATERIALS AND METHODS

Materials. Glasses and aluminum alloy sheets (Al) with dimensions of 60 × 30 × 5 mm^3 (length × width × height) were used for all experiments. A low surface energy silane, 1H,1H,2H,2H-perfluorodecyltrimethoxysilane (Aladdin, China), is adopted for surface modification. The tested lubricant was No. 10 aviation hydraulic oil (density of 850 $kg{\cdot}m^{-3}$, dynamic viscosity of 8.5 mPa·s at 20 °C, surface tension of 33.7 $mN{\cdot}m^{-1}$ at 20 °C). All chemicals are analytically pure and used as received.

Specimen Preparation and Characterization. The surfaces with different roughnesses and wettabilities are fabricated by the same steps as shown in ref 22. The fabrication process is shown in Figure 1a. To avoid the effects of surface contaminants, before the fabrication process, the glasses are immersed in a strong oxidizing solution at 85 °C for 30 min, and then the glasses are ultrasonically cleaned in ethanol for 5 min and dried under N_2, sequentially. The Al alloys are polished via sandpapers (mesh numbers of 36, 100, 200, 500, and 1000) to remove oxidized layers for uniform electrical conductivity. The specimens are ultrasonically cleaned in ethanol for 5 min, etched via anodic electrodisposal (0.1 mol/L sodium chloride), and roughness changed by controlling the dissolution time; the parameters are shown in Table 1. Then, the roughened Al was dipped into boiling water (40 min) for alkaline oxidation to create irregular hierarchical micro- and nanostructures.

The SEM and EDS images (Nova Nano SEM 450, FEI, Japan) in Figure 1b_1−b_4,c_1−c_4 confirm the morphology and component of irregular micro- and nanostructures. After that, the cleaned glass, roughened Al, and the 10 wt % of toluene solution with

Table 1. Parameters for Preparing Irregular Roughened Surfaces with Different Roughnesses

S_a, μm	current density, A/cm^2	dissolving, min	boiling, min	modification, h
~6	0.7	3	40	1/3
~4	0.7	6	40	1/3
~2	0.7	15	40	1/3

https://doi.org/10.1021/acs.langmuir.4c00949
Langmuir 2024, 40, 12842−12851

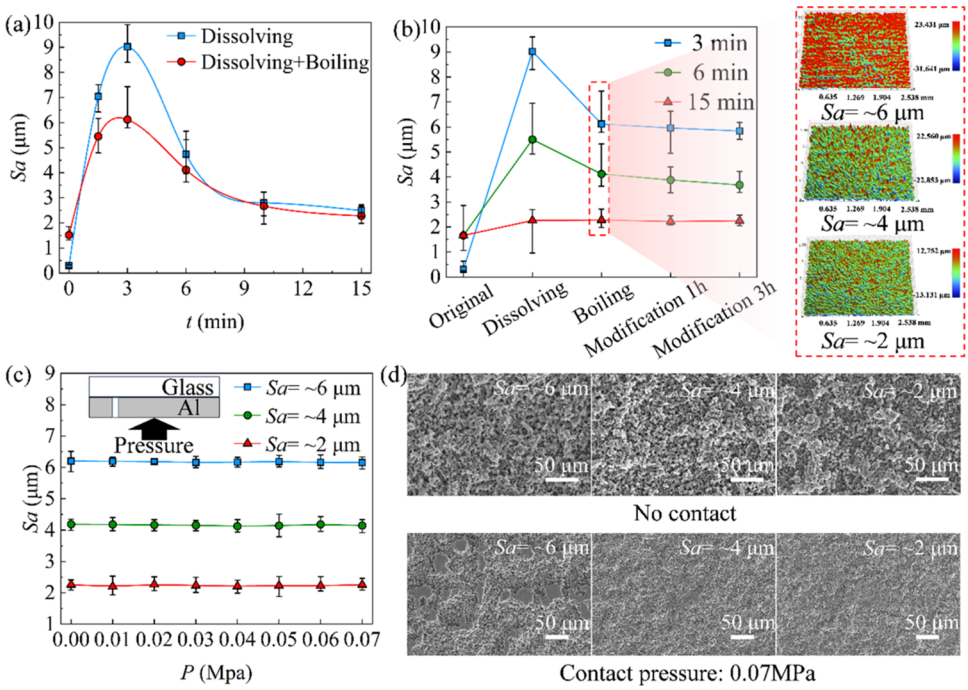

Figure 2. (a) Variation curves of the surface roughness on Al surfaces with time for different treatments. (b) Surface roughness and 3D images of Al after different treatments. (c) Variation curves of the surface roughness on Al surfaces under different contact pressures. (d) SEM images of Al surfaces with different roughnesses under contact pressures of 0 and 0.07 MPa.

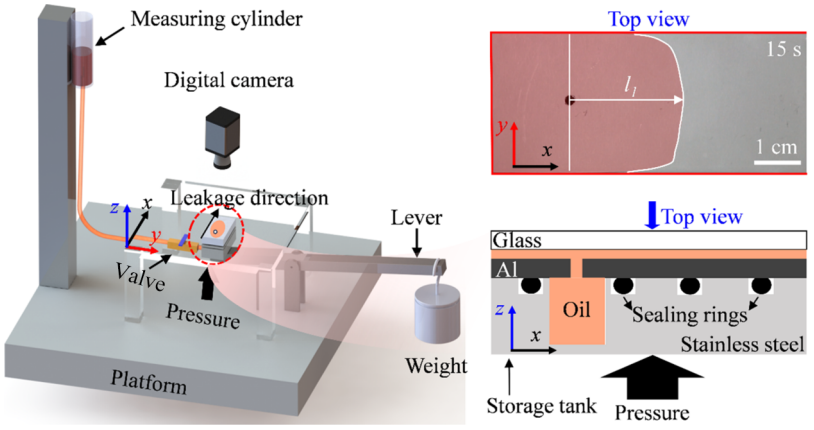

Figure 3. Schematic diagram of the self-design apparatus.

1H,1H,2H,2H-perfluorodecyltrimethoxysilane are put into a sealed jar at 80 °C for 1 and 3 h to achieve surfaces with different wettabilities. The appearance of the F element in Figure 1c$_4$ confirms that the silane was coated on Al successfully. The oil contact angles on the prepared surfaces are measured by a contact angle measuring instrument (SL-200B, Solon, China). Droplets of 5 μL were placed on the surfaces, and images were taken within several seconds after the equilibrium state was reached.

The surface roughness (S_a) is the arithmetic mean deviation based on the height of the entire surface profile, which is used to represent the roughness of all prepared surfaces and is measured by a 3D optical profilometer (Contour GT, Bruker); 5 areas (2.538 × 1.904 mm^2) on the surface were selected for measurement, and the average value was taken, as shown in Figure 2. Figure 2a shows the curves of the S_a of Al surfaces after different treatments with time, the S_a increases and then decreases with the increase of time, and the S_a is at its maximum at 3 min. In addition, the S_a of the surface treated by dissolving and boiling is lower than that of the surface treated by dissolving. In this paper, the dissolving time of 3, 6, and 15 min and the boiling treatment of 40 min were selected for Al surfaces with S_a values of ~6, ~4, and ~2 μm. Figure 2b shows the variation curves of S_a of the Al surfaces after different treatments. After the boiling process, the roughened surfaces of S_a are ~6, ~4, and ~2 μm (Figure 2b). When the roughened surfaces are modified, the S_a of surfaces has no change. To confirm the property of the prepared rough structures, mechanical stability (pressure-resistant) of the prepared surfaces was evaluated via a pressure test. After the roughened surfaces are pressurized by different forces, the S_a is almost unchanged and the stability is acceptable. Figure 2d shows the SEM images of Al surfaces with different roughnesses before and after squeezing comparison, from which it can be seen that the Al surfaces were deformed and flattened when the surfaces were squeezed by a 0.07 MPa contact pressure. Under the same contact pressure, the surface with a roughness of 6 μm was deformed only in the spiked area, while the surface with a roughness of 2 μm was deformed in less areas. No significant effect on surface topography was observed.

Apparatus and Test Procedure. The leakage process and leakage rate are obtained by a self-design apparatus. As shown in Figure 3, a storage tank made of stainless steel with a dimension of 60 mm × 30 mm × 15 mm was connected to a pipe for oil supply from

https://doi.org/10.1021/acs.langmuir.4c00949
Langmuir 2024, 40, 12842−12851

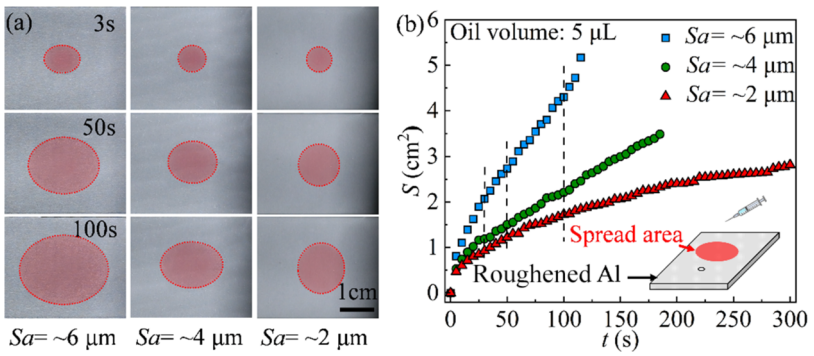

Figure 4. Images (a) and curves (b) of the spreading area of oil on Al surfaces with different roughnesses.

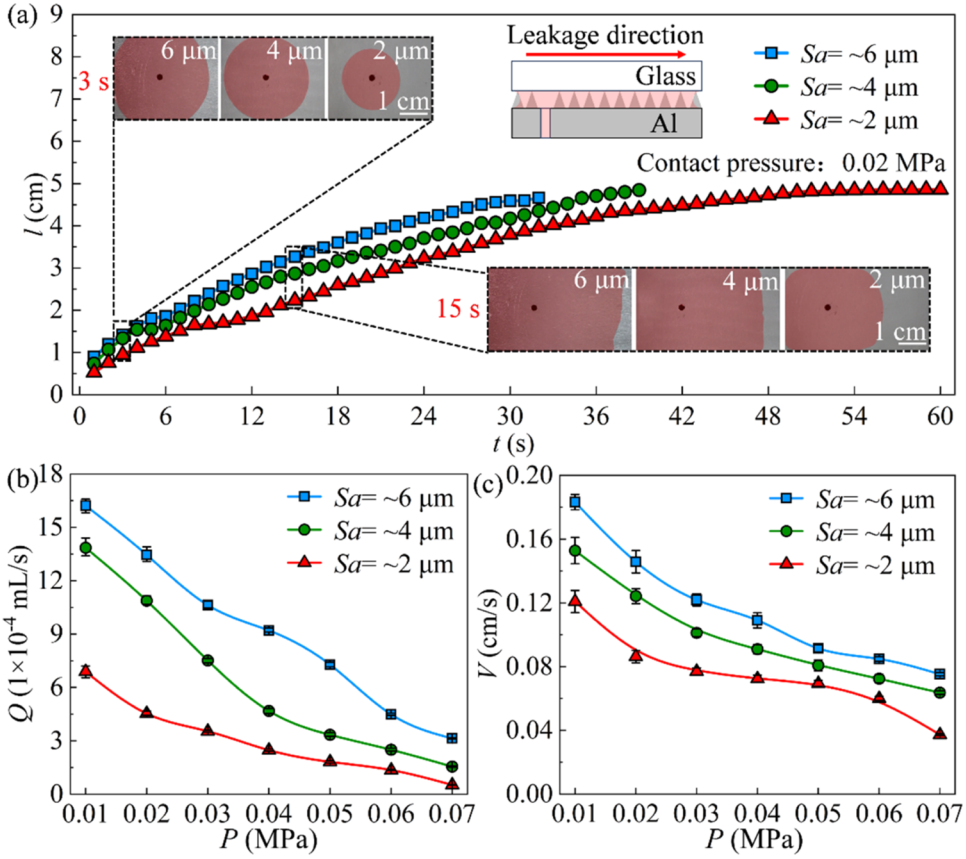

Figure 5. (a) Variation curves of the leakage distance versus time. (b) The leakage rate and (c) leakage velocity in the interface formed by glass and Al with different roughnesses.

the measuring cylinder. A glass and Al alloy plate are mounted on the storage tank. The lever is placed underneath the storage tank, and by applying a specific self-weight, a controlled contact pressure can be generated between the interfaces. The plexiglass plate (poly(methyl methacrylate), PMMA, 100 mm × 100 mm × 10 mm) is used to hold down the glass, and the whole apparatus is fixed to a platform. No. 10 aviation hydraulic oil is used for leakage experiments, and it could flow into the interface of glass and Al plates via the through-hole in the Al plate.

The experiment process is as follows: the aviation hydraulic oil with 30 mL is poured into a measuring cylinder, and then the value is opened to allow the oil to flow into the interface. The leakage process is captured via a digital camera (D750, Nikon, Japan). The leakage rate Q and average velocity of the interface leakage V are calculated as follows

$$Q_{exp} = \frac{V_1 - V_2}{t_1} \quad (1)$$

$$V_{exp} = \frac{l}{t_2} \quad (2)$$

where V_1 is the volume of oil at the beginning, V_2 is the volume of oil at the end, t_1 is the total time of the leakage process, l is the average distance from hole to end on Al (from Figure 3), and t_2 is the time of oil flowing out of the hole to the end. Each test condition is repeated at least three times, and the average values are shown.

RESULTS AND DISCUSSION

Effect of Roughness. To explore the difference of the superoleophilic surfaces with different roughnesses, 5 μL of oil is dropped and spread on Al surfaces with S_a of ~6, ~4, and ~2

https://doi.org/10.1021/acs.langmuir.4c00949
Langmuir 2024, 40, 12842−12851

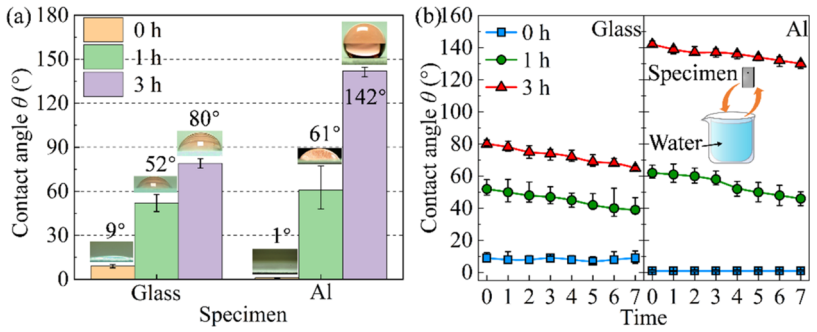

Figure 6. (a) Contact angle of glass and Al modification for different times and (b) variation curves of contact angles of glass and Al with different wettabilities after repeated cleaning.

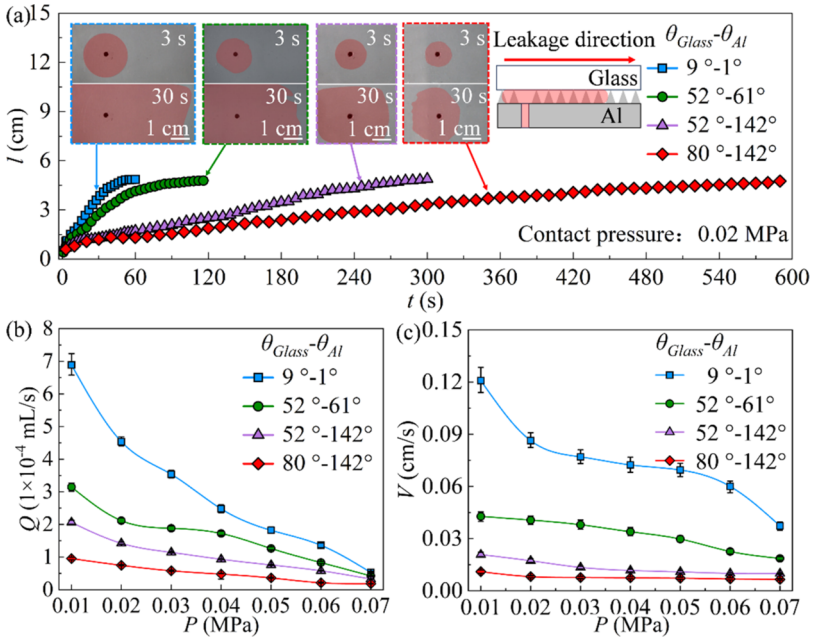

Figure 7. (a) Variation curves of leakage distance versus time. (b) The leakage rate and (c) leakage velocity in the interface formed by glass and Al with different wettabilities.

μm. Figure 4a shows images of oil spreading on the Al surface with different roughnesses after 3, 50, and 100 s. Figure 4b shows the curves of the spreading area of oil on different roughness surfaces with time. As shown in Figure 4a,b, at the same time, the spreading area of oil on the larger roughness surface is larger than that on the smaller roughness surface, which indicates that the oil is easier to spread on the surface with higher roughness. This is due to the fact that when the surface roughness is increased, the capillary effect is stronger, the oil is more easily infiltrated into the surface, and the spreading speed is also accelerated.[27,28]

Figure 5a shows the curves of leakage distance with time in the interface between glass and Al with different roughnesses under a contact pressure of 0.02 MPa. The Al specimens with roughness of ~6, ~4, and ~2 μm are selected as lower specimens in this experiment, and the glass (S_a = ~7 nm) is selected as the upper sample. All selected specimen surfaces were superoleophilic. As shown in Figure 5a, at the same time, the leakage distance of oil in the interface formed by glass and Al (S_a = ~2 μm) is smaller than that of the interface formed by glass and Al (S_a = ~6 μm). In addition, the images of the leakage process also confirm it. As shown in the leakage process, for all interfaces, the oil spreads uniformly from the center to the surroundings, and once the oil reaches the boundary, it is blocked there and starts to spread in the same direction (Movie S1). At the same time, the leakage of oil in the interface formed by glass and the Al with lower roughness is lower than that interface formed by glass and the Al with higher roughness (Movie S2).

Figure 5b,c presents the effect of contact pressure and roughness on the leakage rate (Q) and velocity (V). It can be seen that the contact pressure and roughness affect the leakage performance. As shown in Figure 5b, for the same roughness, the leakage rate decreases with increasing contact pressure. Compared to 0.01 MPa, the leakage rate at 0.07 MPa is reduced by 73, 84, and 90%. For the same contact pressure, the leakage rate increases with increasing roughness. Under a contact pressure of 0.07 MPa, the leakage rate in the interface by glass and Al with a roughness of 2 μm is 83% lower than that in the interface by glass and Al with a roughness of 6 μm. From Figure 5c, the leakage velocity also has a negative correlation with contact pressure and a positive correlation with surface roughness. Compared to 0.01 MPa, the leakage velocity at 0.07 MPa is reduced by 59, 63, and 69%. Under a contact pressure of 0.07 MPa, the leakage velocity in the interface by glass and Al with a roughness of 2 μm is 50%

https://doi.org/10.1021/acs.langmuir.4c00949
Langmuir 2024, 40, 12842−12851

lower than that in the interface by glass and Al with a roughness of 6 μm.

Therefore, for the selection of seals, it is necessary to avoid the selection of surfaces with large roughness that is conducive to leakage.

Effect of Wettability. Before the effect of wettability on leaking performance is investigated, the stability of the wettability should be confirmed. Figure 6 shows the contact angles of glass and Al modification at different times. It can be seen that the oil contact angles of cleaned glass and roughened Al are 9 and 1°, respectively, which are superoleophilic. When the low-energy silane was modified for 1 h, the glass and Al showed oleophilicity and reached 52 and 61°, respectively. When the modification time is further increased, the contact angle reaches 80 and 142°, respectively. The stability of the silane coating is shown in Figure 6b. The glass and Al coated with silane are completely immersed in oil and removed in deionized water for ultrasonic cleaning. With the increase in immersion and cleaning times, the contact angle decreased slightly. It is believed that all prepared surfaces have robust oleophilicity and oleophobicity.

Figure 7a presents the curves of leakage distance with time in the interface between glass and Al with different wettabilities under a contact pressure of 0.02 MPa. As shown in Figure 7a, at the same time, the leakage distance of oil in the interface formed by glass and the Al with superoleophilicity is the largest. As the glasses and Al surfaces change from oleophilicity to oleophobicity, their leakage distances gradually decrease. When the glass has a contact angle of 80° and Al has a contact angle of 142°, its leakage distance is the smallest. In addition, the leakage process also confirms it. At the same time, the leakage of oil in the interface formed by glass and the Al with superoleophilic is faster than others (Movie S3).

Figure 7b,c shows the leakage results between the interface of glass and Al with different wettabilities. It can be seen that the wettability has a significant influence on the leakage performance. As shown in Figure 7b, under the contact pressure of 0.01 MPa, the leakage rate of an interface formed by the glass with a contact angle of 80° and Al with a contact angle of 142° is 83% lower than that interface formed by the glass and Al with superoleophilicity. Under the contact pressure of 0.07 MPa, the leakage rate of interface formed by the glass and Al with superoleophilicity is 64% higher than that interface formed by the glass with a contact angle of 80° and Al with a contact angle of 142°. Figure 7c are consistent with those in Figure 4b. At the same contact pressure, the interface formed by the glass and Al with superoleophilic has the highest leakage velocity. Under the contact pressure of 0.07 MPa, the leakage velocity of interface formed by the glass and Al with superoleophilicity is 82% higher than that interface formed by the glass with a contact angle of 80° and Al with a contact angle of 142°. Therefore, oleophobic surfaces are suggested to delay the leakage.

The experimental results presented above show that wettability has a significant effect on leakage performance. A theoretical model will be developed below to predict the effect of wettability on leakage performance.

Theoretical Model. Figure 8 shows the schematic of oil in the interface formed by a surface with different surface roughnesses and wettabilities. When two surfaces are extruded together, contact does not occur at every point, and microconvexities at the contact interface extrude against each other, thus resulting in gap. The cross section of the oil in the

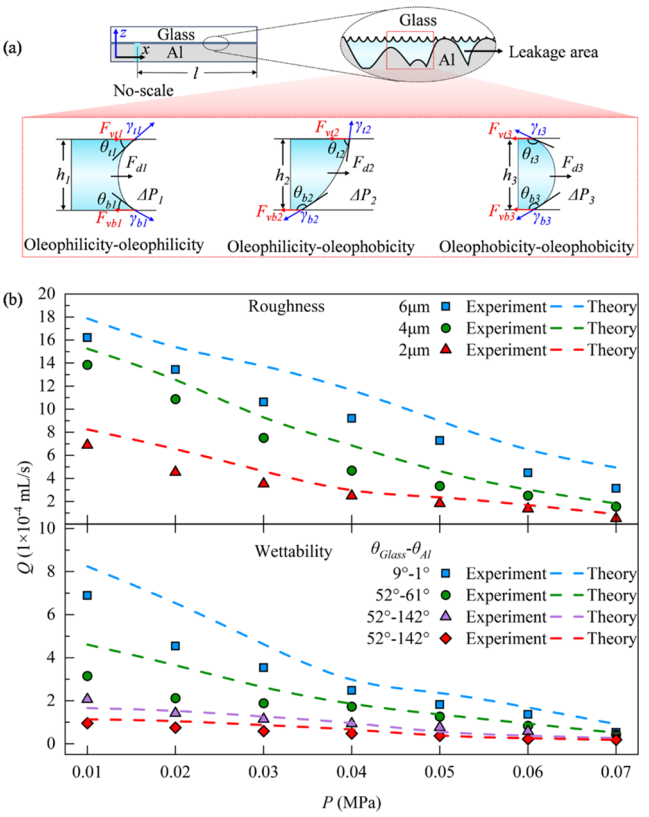

Figure 8. (a) Schematic of oil in the interface formed by surface with different wettabilities. (b) Comparison between the theoretical predictions of the leakage rate in the interface formed by surfaces with different roughnesses and wettabilities and the experimental results.

$x-z$ direction is chosen as a reference. In this paper, based on the fact that wettability reflects surface roughness, a theoretical model for predicting the leakage rate is developed based on the Navier−Stokes equations, and the relationship between the leakage rate and the wettability and roughness is obtained by adding the surface wettability theory to the Navier−Stokes equations.

The relationship between the pressure drop ΔP and velocity $\overline{u}$ can be described by a simplified Navier−Stokes equation as follows[29]

$$\mu\frac{\partial^2 V_x}{\partial z^2} = \frac{\partial P}{\partial x} = -\frac{\Delta P}{l} \tag{3}$$

Integrating and applying the boundary conditions ($z = \frac{h}{2}$, $u = 0$; $z = -\frac{h}{2}$, $u = 0$) given in eq 3, we arrive at the relationship between velocity $\overline{u}$ and ΔP

$$\overline{u} = \frac{Q}{S} = \frac{\Delta P h^2}{12\mu l} \tag{4}$$

The relationship between the leakage rate Q and ΔP can be described as follows

$$Q = \frac{\Delta P h^2}{12\mu l}\cdot S \tag{5}$$

where ΔP is the pressure drop between the inside and outside of oil, h is the gap height between the two surfaces, h between surfaces of different roughnesses is also different, μ is the

https://doi.org/10.1021/acs.langmuir.4c00949
Langmuir 2024, 40, 12842−12851

dynamic viscosity of the oil, S is the cross-sectional area of oil in the $y-z$ direction, and l is the leakage distance of oil in the x direction.

In this study, the pressure drop ΔP consists of 3 components, the pressure gradient due to hydrostatic pressure ($\Delta P_{\text{Hydrostatic}}$), the pressure gradient due to microcapillarity ($\Delta P_{\text{Capillary}}$), and the viscous pressure gradient between oil and interface (ΔP_{v}) during the leakage process, which can be described as follows

$$\Delta P = \Delta P_{\text{Hydrostatic}} + \Delta P_{\text{Capillary}} - \Delta P_{\text{v}} \tag{6}$$

For the pressure gradient of $\Delta P_{\text{Hydrostatic}}$, the initial pressure gradient of oil ΔP_{d} can be described as follows

$$\Delta P_{\text{Hydrostatic}} = \Delta P_{\text{d}} = \rho g \Delta h \tag{7}$$

where ρ is the density of oil, g is the acceleration of gravity, and Δh is the liquid height difference in the graduated cylinder.

For the pressure gradient of $\Delta P_{\text{Capillary}}$, the oil is subjected to the surface tension of the curved liquid−gas interface f. As surface wettability changes, the magnitude and direction of surface tension also change; thus, interfaces with different wettabilities need to be discussed separately.

The surface tension of the curved liquid−gas interface can be described as follows

$$f_{\text{t}} = \gamma L_{\text{t}} \cos\theta_{\text{t}}, \quad f_{\text{b}} = \gamma L_{\text{b}} \cos\theta_{\text{b}} \tag{8}$$

where L_{t} is the perimeter of the wetting area on the glass surface, L_{b} is the perimeter of the wetting area on the Al surface, and θ_{t} and θ_{b} are the contact angles of the upper and lower plates, respectively.

For oil in the interface formed by both surfaces with oleophilicity. The pressure drop $\Delta P_{\text{Capillary1}}$ of oil can be described as follows

$$\Delta P_{\text{Capillary1}} = \frac{(f_{\text{t}} + f_{\text{b}})}{S} = \frac{\gamma(L_{\text{t}}\cos\theta_{\text{t}} + L_{\text{b}}\cos\theta_{\text{b}})}{S} \tag{9}$$

For oil, the interface is formed by one surface with oleophilicity and another surface with oleophobicity. The pressure drop $\Delta P_{\text{Capillary2}}$ of oil can be described as follows

$$\Delta P_{\text{Capillary2}} = \frac{(f_{\text{t}} - f_{\text{b}})}{S} = \frac{\gamma(L_{\text{t}}\cos\theta_{\text{t}} - L_{\text{b}}\cos\theta_{\text{b}})}{S} \tag{10}$$

For oil in the interface formed by both surfaces with oleophobicity, the pressure drop $\Delta P_{Capillary3}$ of oil can be described as follows

$$\Delta P_{\text{Capillary3}} = -\frac{(f_{\text{t}} + f_{\text{b}})}{S} = -\frac{\gamma(L_{\text{t}}\cos\theta_{\text{t}} + L_{\text{b}}\cos\theta_{\text{b}})}{S} \tag{11}$$

For the pressure gradient of ΔP_{v}.

Based on Newton's viscosity law, the viscous force F_{v} can be described as follows[30]

$$F_{\text{v}} = A \cdot \mu \cdot \frac{\text{d}u}{\text{d}y} \tag{12}$$

where A is the contact area, μ is the dynamic viscous coefficient, and $\frac{\text{d}u}{\text{d}y}$ is the velocity gradient.

The ΔP_{v} can be described on the basis of the F_{v} as

$$\Delta P_{\text{v}} = \Delta P_{\text{vt}} + \Delta P_{\text{vb}} = \frac{F_{\text{vt}} + F_{\text{vb}}}{S} = \frac{A_{\text{t}} \cdot \mu_{\text{t}}}{S} \cdot \frac{\text{d}u_{\text{t}}}{\text{d}y} + \frac{A_{\text{b}} \cdot \mu_{\text{b}}}{S} \cdot \frac{\text{d}u_{\text{b}}}{\text{d}y} \tag{13}$$

where ΔP_{vt} is the pressure gradient between the oil and the top surface, and ΔP_{vb} is the pressure gradient between the oil and the bottom surface.

Substituting ΔP from eqs 7, 9, 10, 11, and 13 into eq 6. The ΔP for different wettability interfaces can be obtained

$$\Delta P_{\text{oleophilic-oleophilic}} = \Delta P_{\text{Hydrostatic}} + \Delta P_{\text{Capillary1}} - \Delta P_{\text{v}} = \rho g \Delta \text{h} + \frac{\gamma(L_{\text{t}}\cos\theta_{\text{t}} + L_{\text{b}}\cos\theta_{\text{b}})}{S} - \left(\frac{A_{\text{t}} \cdot \mu_{\text{t}}}{S} \cdot \frac{\text{d}u_{\text{t}}}{\text{d}y} + \frac{A_{\text{b}} \cdot \mu_{\text{b}}}{S} \cdot \frac{\text{d}u_{\text{b}}}{\text{d}y}\right) \tag{14}$$

$$\Delta P_{\text{oleophilic-oleophobic}} = \Delta P_{\text{Hydrostatic}} + \Delta P_{\text{Capillary2}} - \Delta P_{\text{v}} = \rho g \Delta \text{h} + \frac{\gamma(L_{\text{t}}\cos\theta_{\text{t}} - L_{\text{b}}\cos\theta_{\text{b}})}{S} - \left(\frac{A_{\text{t}} \cdot \mu_{\text{t}}}{S} \cdot \frac{\text{d}u_{\text{t}}}{\text{d}y} + \frac{A_{\text{b}} \cdot \mu_{\text{b}}}{S} \cdot \frac{\text{d}u_{\text{b}}}{\text{d}y}\right) \tag{15}$$

$$\Delta P_{\text{oleophobic-oleophobic}} = \Delta P_{\text{Hydrostatic}} + \Delta P_{\text{Capillary3}} - \Delta P_{\text{v}} = \rho g \Delta \text{h} - \frac{\gamma(L_{\text{t}}\cos\theta_{\text{t}} + L_{\text{b}}\cos\theta_{\text{b}})}{S} - \left(\frac{A_{\text{t}} \cdot \mu_{\text{t}}}{S} \cdot \frac{\text{d}u_{\text{t}}}{\text{d}y} + \frac{A_{\text{b}} \cdot \mu_{\text{b}}}{S} \cdot \frac{\text{d}u_{\text{b}}}{\text{d}y}\right) \tag{16}$$

Substituting ΔP from eqs 14−16 into eq 5. One could easily predict the leakage rate

$$Q = \begin{cases} \dfrac{\Delta P_{\text{oleophilic-oleophilic}} \cdot h^2}{12\mu l} \cdot S, & \theta_{\text{t}}, \theta_{\text{b}} < 90^\circ \\ \dfrac{\Delta P_{\text{oleophilic-oleophobic}} \cdot h^2}{12\mu l} \cdot S, & \theta_{\text{t}} < 90^\circ,\ \theta_{\text{b}} > 90^\circ \\ \dfrac{\Delta P_{\text{oleophobic-oleophobic}} \cdot h^2}{12\mu l} \cdot S, & \theta_{\text{t}}, \theta_{\text{b}} > 90^\circ \end{cases} \tag{17}$$

Verification. In what follows, a comparison of theoretical and experimental values of the leakage rate in the interface is formed by surfaces with different roughnesses and wettabilities. Equation 17 can be used to predict the leakage rate in different interfaces.

Figure 8b shows both the theoretical and experimental results for the leakage rate of oil in the interface formed by surfaces with different roughnesses and wettabilities. As shown in Figure 8b, the leakage rate is negatively correlated with the contact pressure and positively correlated with surface roughness. In addition, the leakage rate of oil in the interface formed by surfaces with oleophilicity is higher than that of oil

https://doi.org/10.1021/acs.langmuir.4c00949
Langmuir 2024, 40, 12842−12851

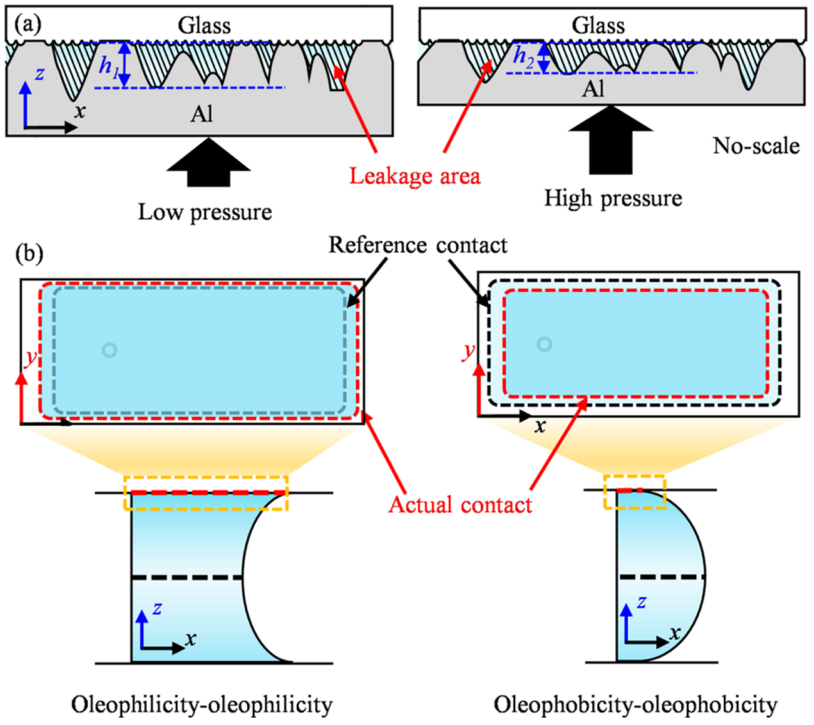

Figure 9. Schematic mechanism of the effect of roughness (a) and wettability (b) on leakage performance.

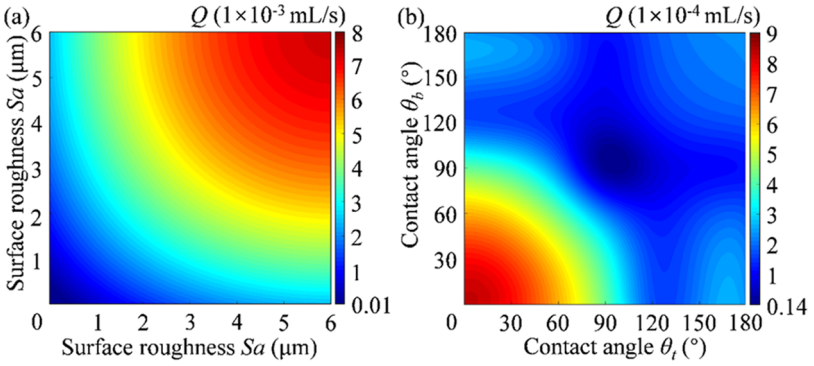

Figure 10. Leakage rate distribution with surface roughness (a) and contact angle (b).

in the interface formed by surfaces with oleophobicity. In general, the experimental data fit the theory results well, and the trend of change is consistent, which further establishes the validity of the theoretical model.

Mechanism. To understand more easily the effect of contact pressure, roughness, and wettability on the leakage performance, Figure 9 and eq 17 can be used to explain that, as can be seen from Figure 9a; when the two seal surfaces come into contact, they are not in complete contact, and some gaps appear, which make up leakage channels that can be leaked. When a load is applied to the contact surfaces, which causes the contact points to be further squeezed or even deformed (Figure 2d), the height and volume of these leakage channels are reduced or even disappear, thus reducing the leakage. In addition, the height of the leakage channel also depends on the processing method and surface roughness of the contact surface, the greater the surface roughness, the greater the volume of the leakage channel, the greater the height of the gap; according to eq 17, the leakage rate and the height of the gap are positive with surface roughness, that is, the greater the surface roughness is, the greater the leakage rate will be.

Figure 9b shows a schematic diagram to explore the effect of wettability on leakage performance. Figure 8a can also help us to better understand, from Figures 8a and 9b, that when the sealing surface is oleophilic, the oil in the two contact surfaces subjected to the surface tension is conducive to the leakage of the oil. With the increase of the contact angle, surface tension in the parallel direction is decreased, and the leakage rate is also decreased. When the contact angle reaches 90°, the surface tension in the parallel direction is 0. When the contact angle increases further, the direction of surface tension is altered in a direction opposite to the direction of leakage and gradually increases. However, compared with the oleophilic surface, the actual contact area and contact perimeter of the oil on the oleophobicity surface decrease with the increase of the contact angle, and thus the viscous force decreases, which leads to the leakage rate slowly becoming larger when the contact angle is greater than 90°.

Therefore, leakage can be delayed by reducing surface roughness, increasing the suitable contact pressure, and selecting oleophobicity surfaces that have a contact angle of 90−110°.

https://doi.org/10.1021/acs.langmuir.4c00949
Langmuir 2024, 40, 12842−12851

Predictions. Equation 17 can be used to predict the variation of leakage rate in interfaces formed by surfaces with different wettabilities. Figure 10 exhibits the leakage rate distribution with surface roughness and contact angle. As shown in Figure 10a, as the surface roughness of the seal surface increases, the leakage rate also increases. From Figure 10b, the contact angle increases from 0°, and the leakage rate shows a decreasing trend; when the contact angle reaches about 94°, the leakage rate reaches the minimum at this time, but when the contact angle continues to increase, the leakage rate begins to increase. Therefore, for the selection of sealing surfaces, the low roughness surfaces and oleophobicity surfaces with a contact angle of 90−110° can be considered.

CONCLUSIONS

In the research of static seals, many experiments and models about surface parameters have been proposed to lay the foundation for further enriching the theory of static seals.[10,12−21] However, considering that the leakage channel formed at the seal interface is only a micrometer in size, which belongs to the category of microflow, the neglect of surface properties has a great impact on the prediction of leakage rate.[31] Based on this, the effects of contact pressure, roughness, and wettability on the leakage performance in static seal systems are investigated, where surfaces with different roughnesses and wettabilities are prepared by fabricating roughened structures and modifying low surface energy. The leakage processes are captured. Our experimental study revealed that contact pressure, roughness, and wettability have a significant effect on the leakage performance, the leakage rate is negatively correlated with contact pressure and positively correlated with roughness, and the leakage rate of the interface formed by oleophobicity surfaces is lower than that of the interface formed by oleophilicity surfaces. In addition, a theoretical model based on wettability is developed to predict the trend of leakage rate under the variation of different roughnesses and contact angles, which is crucial for the improvement of seal theory in modern machinery.

ASSOCIATED CONTENT

Supporting Information

The Supporting Information is available free of charge at https://pubs.acs.org/doi/10.1021/acs.langmuir.4c00949.

Movie captions of the leakage process (PDF)

Oil leak in the interface between glass and Al under a contact pressure of 0.02 MPa (Movie S1) (MP4)

Oil leak in the interfaces between glass and Al with different roughnesses (Movie S2) (MP4)

Oil leak in the interfaces between glass and Al with different wettabilities (Movie S3) (MP4)

AUTHOR INFORMATION

Corresponding Author

Qingwen Dai − *College of Mechanical and Electrical Engineering, Nanjing University of Aeronautics and Astronautics, Nanjing 210016, China;* orcid.org/0000-0001-7422-4259; Email: daiqingwen@nuaa.edu.cn

Authors

Zhengpeng Gu − *College of Mechanical and Electrical Engineering, Nanjing University of Aeronautics and Astronautics, Nanjing 210016, China*

Chenbo Ma − *School of Mechanical and Electrical Engineering, Nanjing Forestry University, Nanjing 210037, China*

Wei Huang − *College of Mechanical and Electrical Engineering, Nanjing University of Aeronautics and Astronautics, Nanjing 210016, China*

Xiaolei Wang − *College of Mechanical and Electrical Engineering, Nanjing University of Aeronautics and Astronautics, Nanjing 210016, China;* orcid.org/0000-0002-9055-1011

Complete contact information is available at: https://pubs.acs.org/10.1021/acs.langmuir.4c00949

Author Contributions

[§]Z.G. and Q.D. contributed equally to this work.

Notes

The authors declare no competing financial interest.

ACKNOWLEDGMENTS

The authors are grateful for the support provided by the National Natural Science Foundation of China (Nos. 52175172 and 51805252).

REFERENCES

(1) Shabbir, S.; Garvey, S. D.; Dakka, S. M.; Rothwell, B. C. Seal failure in aerospace application-creating a global open-source database. *Seal. Technol.* **2021**, *2*, 7−9.

(2) Zhang, J.; Hu, Y. Mechanical behavior and sealing performance of metal sealing system in roller cone bits. *J. Mech. Sci. Technol.* **2019**, *33* (10), 2855−2862.

(3) Zhang, Q.; Chen, X. Q.; Huang, Y. Y.; Zhang, X. An Experimental Study of the Leakage Mechanism in Static Seals. *Appl. Sci.* **2018**, *8* (8), 1404.

(4) Ledoux, Y.; Lasseux, D.; Favreliere, H.; Samper, S.; Grandjean, J. On the dependence of static flat seal efficiency to surface defects. *Int. J. Pressure Vessels. Pip.* **2011**, *88*, 518−529.

(5) Murtagian, G. R.; Fanelli, V.; Villasante, J.; Johnson, D.; Ernst, H. Sealability of stationary metal-to-metal seals. *J. Tribol.* **2004**, *126* (3), 591−596.

(6) Yanagisawa, T.; Sanada, M.; Koga, T.; Hirabayashi, H. The Influence of Designing Factors on the Sealing Performance of C-Seal. *SAE Trans.* **1991**, *100*, 651−657, DOI: 10.4271/910535.

(7) Goltsberg, R.; Gilad, M. Experimental study of the sealing performance of metal on polymer conical seals. *J. Tribol.* **2022**, *144*, No. 062303.

(8) Ou, J.; Perot, B.; Rothstein, J. P. Laminar drag reduction in microchannels using ultrahydrophobic surfaces. *Phys. Fluids* **2004**, *16* (12), 4635−4643.

(9) Choi, C. H.; Westin, K. J. A.; Breuer, K. S. Apparent slip flows in hydrophilic and hydrophobic microchannels. *Phys. Fluids* **2003**, *15* (10), 2897−2902.

(10) Heinze, E. Besonderer BerÜcksichti-dung ihrer Verwendung im Kältema schinenbau. *Kältetechnik* **1949**, *1*, 26−32.

(11) Mayer, E. *Mechanical Seals*; Chemical Industry Press, 2013.

(12) Lebeck, A. O. Hydrodynamic lubrication in wavy contacting face seals-a two dimensional model. *J. Lubr. Technol.* **1981**, *103* (4), 578−586.

(13) Elhanafi, S.; Farhang, K.In *Leakage Prediction in Mechanical Seals Under Hydrostatic Operating Condition*, International Joint Tribology Conference, 2007; pp 505−507.

(14) Lebeck, A. Contacting mechanical seal design using a simplified hydrostatic model. *Tribol. Int.* **1988**, *21* (1), 2−14.

(15) Lorenz, B.; Persson, B. Leak rate of seals: Comparison of theory with experiment. *Europhys. Lett.* **2009**, *86* (4), 44006.

(16) Campañá, C.; Persson, B.; Müser, M. Transverse and normal interfacial stiffness of solids with randomly rough surfaces. *J. Phys.: Condens. Matter* **2011**, *23* (8), No. 085001.
(17) Persson, B. N. J.; Yang, C. Theory of the leak-rate of seals. *J. Phys.: Condens. Matter* **2008**, *20* (31), No. 315011.
(18) Persson, B. N. J.; Albohr, O.; Creton, C.; Peveri, V. Contact area between a viscoelastic solid and a hard, randomly rough, substrate. *J. Chem. Phys.* **2004**, *120* (18), 8779−8793.
(19) Majumdar, A.; Bhushan, B. Fractal model of elastic-plastic contact between rough surfaces. *J. Tribol.* **1991**, *113* (11), 1−11.
(20) Sun, J. J.; Wei, L.; Feng, X.; Gu, B. Q. Leakage prediction method for contacting mechanical seals with parallel faces. *Chin. J. Mech. Eng.* **2010**, *23* (1), 7.
(21) Bottiglione, F.; Carbone, G.; Mantriota, G. Fluid leakage in seals: An approach based on percolation theory. *Tribol. Int.* **2009**, *42* (5), 731−737.
(22) Chen, S. Q.; Dai, Q. W.; Yang, X. L.; Liu, J.; Huang, W.; Huang, W.; Wang, X. L. Bioinspired Functional Structures for Lubricant Control at Surfaces and Interfaces: Wedged-Groove with Oriented Capillary Patterns. *ACS Appl. Mater. Interfaces* **2022**, *14*, 42635−42644.
(23) Qi, B.; Yang, X. L.; Wang, X. L. Ultraslippery/hydrophilic patterned surfaces for efficient fog harvest. *Colloids Surf., A* **2022**, *640*, No. 128398.
(24) Yang, X. L.; Qi, B.; Lu, Y.; Zhang, W.; Wang, X. L. Bionic surface diode for droplet steering. *Droplet* **2023**, *2*, No. e46, DOI: 10.1002/dro2.46.
(25) Yang, X. L.; Zhuang, K.; Lu, Y.; Wang, X. L. Creation of Topological Ultraslippery Surfaces for Droplet Motion Control. *ACS Nano* **2021**, *15*, 2589−2599.
(26) Zhou, X.; Sheng, J. L.; Ye, Z. Y. Evaluation of immiscible two-phase quasi-static displacement flow in rough fractures using LBM simulation: Effects of roughness and wettability. *Capillarity* **2024**, *11*, 41−52.
(27) Dai, Q. W.; Huang, W.; Wang, X. L. Surface roughness and orientation effects on the thermo-capillary migration of a droplet of paraffin oil. *Exp. Therm. Fluid Sci.* **2014**, *57*, 200−206.
(28) Dai, Q. W.; Li, M.; Khonsari, M. M.; Huang, W.; Wang, X. L. The thermocapillary migration on rough surfaces. *Lubr. Sci.* **2019**, *31*, 163−170.
(29) Zhuang, K.; Lu, Y.; Wang, X. L.; Yang, X. L. Architecture-Driven Fast Droplet Transport without Mass Loss. *Langmuir* **2021**, *37* (43), 12519−12528.
(30) Yang, X. L.; Liu, X.; Lu, Y.; Song, J. L.; Huang, S.; Zhou, S.; Jin, Z. J.; Jin, Z.; Xu, W. J. Controllable Water Adhesion and Anisotropic Sliding on Patterned Superhydrophobic Surface for Droplet Manipulation. *J. Phys. Chem. C* **2016**, *120* (13), 7233−7240.
(31) Zheng, W.; Sun, J. J.; Ma, C. B.; Yu, Q. P. Interface Leakage Theory of Mechanical Seals Considering Microscopic Forces. *Coatings* **2023**, *13* (8), 1435.

https://doi.org/10.1021/acs.langmuir.4c00949
Langmuir 2024, 40, 12842−12851